CrossMark

ORIGINAL PAPER

Controllable Synthesis of Covellite Nanoparticles via Thermal Decomposition Method

F. Davar[1] · M. R. Loghman-Estarki[2] ·
M. Salavati-Niasari[3] · M. Mazaheri[4]

Abstract In this study, covellite (CuS) nanoparticles were synthesized through a facile and low temperature thermal decomposition method using $[Cu(sal)_2]$- oleylamine complex, (sal = salicylaldehydeato, prepared in situ from $[Cu(sal)_2]$ and oleylamine as the precursors), and sulfur as the Cu^{2+} source and S source, respectively. Scanning electron microscope, transmission electron microscope, electron diffraction and ultraviolet–visible absorption (UV–Vis) spectra were used for the characterization of the products. The effect of reaction parameters, such as the copper:sulfur molar ratio, the reaction temperature and the reaction time on the shape, size and phase of CuS nanostructures, was investigated. The results showed that the, covellite (hexagonal structure of CuS) with an average size between 20 and 45 nm could be obtained with the Cu:S molar ratio of 1: 3 at 105 °C for 60 min. With increasing the reaction temperature from 105 to 200 °C, non-stoichiometric $Cu_{1.65}S$ with the average size of 25–50 nm was obtained due to the different existing state of the released Cu^{2+} ions from the copper-oleylamine complex.

Keywords Covellite · CuS · Nanostructures · Chemical synthesis

✉ F. Davar
davar@cc.iut.ac.ir

[1] Department of Chemistry, Isfahan University Of Technology, Isfahan, Islamic Republic of Iran

[2] Department of Material Engineering, Malek Ashtar University of Technology, Isfahan, Iran

[3] Institute of Nano Science and Nano Technology, University of Kashan, Kashan, Islamic Republic of Iran

[4] Advanced Materials Research Center, Poly Techniques University of EPFL, Lucan, Switzerland

Introduction

Copper sulfides are an interesting class of metal sulfides with variable stoichiometries, such as CuS, $Cu_{1.75}S$, $Cu_{1.8}S$, $Cu_{1.94}S$, $Cu_{1.96}S$, Cu_7S_4 and Cu_2S [1]. Some Copper sulfides with variable composition have been identified as p-type semiconducting materials due to copper vacancies within the lattice, which is responsible for their usefulness as optoelectronic materials. Copper sulfides are an important for use as catalysts, coatings, solar cells, optical filters, and so on [2].

Recently, controlling the sizes and morphologies of CuS and metal sulfide nanostructures has been found to be very important in order to enhance the physicochemical properties of this semiconductor [3, 4]. Many methods have been developed to synthesize nanoparticles, wires, belts, tubes, spherical and hollow copper and metal sulfides. These methods are such as solid state reaction [5–7], spray pyrolysis deposition [8], ultrasonic sonochemistry [9], solvothermal and hydrothermal synthesis [10–13], wet chemical route [14–17] and thermolysis [18].

The preparation of metal oxides and metal sulfide nanostructures through thermal decomposition of complexes is an attractive area for chemists, since there have many advantages such as the control of process conditions, particle size, particle crystal structure, and purity [19–23]. Molecular precursors have been used to prepare Cu_xS. Inoue et al. obtained the amorphous CuS nanostructure with $[Cu(en)_2]^{+2}$, (en = ethylenediamine), and thiourea as the precursor [23]. Paul et al. synthesized CuS by decomposing complex $Cu_4(S_5)(N-MeIm)_4$ (N-MeIm = N-methylimidazole) at 500 °C [24]. Chen et al. synthesized copper sulfide nanoparticles by solvothermal decomposition of (copper dialkyldithiophosphates) at 120–200 °C [25].

One potentially attractive chemical method to prepare metal sulfides is thermal decomposition. In this technique, the selection of good surfactant, solvent and sulfur source is the key parameter. Moreover, the advantages of using solvents such as oleylamine to prepare colloidal nanoparticles have attracted much attention [26–29]. Chin et al. successfully synthesized copper sulfide nanoparticles via the decomposition of an-air stable precursor, copper(I) thiobenzoate, in the presence of dodecanethiol [30]. Chen et al. reported CuS nanodisk by thermal decomposition [31].

Korgel [21] synthesized CuS nanodisks by the reaction of copper(II) acetylacetonate with elemental sulfur in o-dichlorobenzene using oleyamine and octanoic acid as the surfactant at 182 °C for 60 min. L. Gao [22] prepared CuS flakes in a quaternary by microemulsion of $CTAB/n-C_5H_{11}OH/n-C_6H_{14}$/water containing copper and sulfur precursors at 130 °C for 15 h. Here, we have reported the use of thermal decomposition method by employing an inorganic precursor $[Cu(sal)_2]$ to synthesize hexagonal CuS (Covellite) nanoparticles under mild condition. Herein, it has been shown that this method was simple, template-free and low temperature (105 °C for 1 h) method for synthesizing covellite nanostructures. The ratios of the starting reagents, including organometallic compounds, surfactant, and solvent, are the key parameters for the control of the size and the morphology of metal sulfide nanoparticles. The reaction temperature as well as the reaction time could also be crucial for the precise control of size and morphology.

Experimental

Materials

Organometalic precursor; [bis(salicylaldehydeato)copper(II)]; was prepared in similar manner to that reported previously [32]. Oleylamine; (Technical grade), elemental sulfur; (99.95 %), absolute ethanol were analytical grade and purchased from Fluka Co. All reagents were used without further treatment.

Typical Synthetic Process of Copper Sulfide Nanoparticles

CuS nanoparticles were synthesized in a three-neck flask under argon atmosphere. [Cu(sal)$_2$]-oleylamine complex was prepared by reacting 2 mmol of [Cu(sal)$_2$] solution and 10 ml of oleylamine. The mixed solution was placed into a flask under stirring and heating and then 2 mmol of elemental sulfur was injected into the complex. The complex was rapidly heated up to 105–200 °C and then kept for 60–180 min. During the process, the color of the solution turned from dark green to dark gray. The change in the color indicated the formation of copper sulfides. The solution was then cooled to room temperature and mixed with an excess amount of ethanol used to wash and purify as-obtained copper sulfide nanoparticles. The black suspension was separated by centrifugation and washed with absolute ethanol at least three times. The obtained black solid was dried in a vacuum oven at room temperature.

To investigate the effect of reaction times on the phase and particle size of the product, the 1:3 molar ratio of [Cu(sal)$_2$]:S in oleylamine was kept at 105 °C for 60, 90 and 180 min. Moreover, different reaction temperatures were achieved by heating the solution of 1:3 molar ratio of [Cu(sal)$_2$]:S in 10 mL oleylamine for 1 h at 105, 180 and 200 °C, respectively.

Characterization

The X-ray diffraction (XRD) analyses were performed using a Rigaku D-max C III, X-ray diffractometer using Ni-filtered Cu Kα radiation in the 2θ range of 20°–80°. The scanning electron microscopy (SEM) images were obtained on Philips XL-30ESEM equipped with an energy dispersive X-ray spectroscopy. The transmission electron microscopy (TEM) images and electron diffraction (ED) patterns were obtained on a Hitachi H-800 transmission electron microscope at an acceleration voltage of 200 kV. UV–Vis absorption spectrum was recorded on a Shimadzu UV-1550 spectrophotometer by dispersing the sample in ethanol at room temperature. Moreover, for comparison of bandgap of nanosized CuS with its microsized (bulk), the one sample was prepared with Pulse Electrical Explosion (PEE) (Nano Engineering and Manufacturing Company, PNF Co., Model: PEE50K, made in Iran). Fourier transform infrared (FT–IR) spectra were recorded with a Shimadzu Varian 4300 spectrophotometer in KBr pellets at room temperature.

Results and discussion

The XRD patterns of the as-products have been shown in Fig. 1. All reflections in Fig. 1a, b (copper:sulfur ratios: (a) 1:3 and (b) 1:5 in 10 mL oleylamine at 105 °C for 60 min) could be indexed to the covellite CuS phase [JCPDS No. 79-2321] with the hexagonal structure. No other impurities such as Cu_2S, oxide or organic compounds were found on the products, thereby indicating that the synthesized
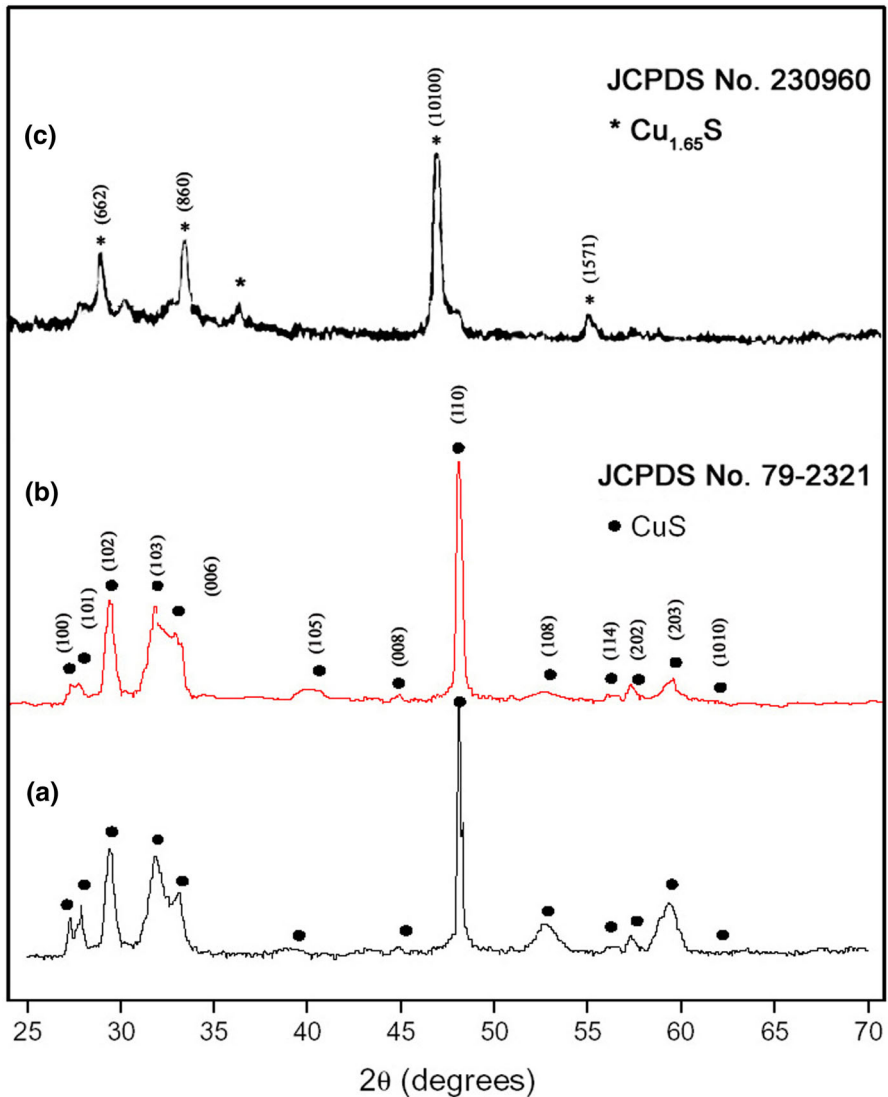
Fig. 1 The XRD patterns of the as-prepared nanoparticles obtained for different temperatures and molar ratios of Cu:S *a* 1:3 obtained at 105 °C, *b* 1:5 obtained at 105 °C and *c* 1:3 at 200 °C for 60 min

(covellite) CuS nanoparticles were pure. The average crystallite size of the copper sulfide nanoparticle was estimated to be 15 nm (Fig. 1a, b), according to the Debye–Scherrer formula [33]. When the reaction temperature was increased from 105 °C (Fig. 1a, b) to 200 °C (Fig. 1c), the crystal phase and composition of the as-obtained nanoparticle were changed. All reflections of Fig. 1c could be indexed as the (digenite) $Cu_{1.65}S$ crystal phase [JCPDS file No. 230960]. The transformation of (covellite) CuS to (digenite) $Cu_{1.65}S$, by increasing reaction temperature could be attributed to the different release rate of the copper from the copper-oleylamine complex [33, 34]. The release rate of sulfur ions was faster than that of copper ions. Furthermore, sulfur ions could exist in various states and combine with copper ions to form copper sulfide; they could also be oxidized to form sulfur and sulfurated hydrogen [33, 34]. At high temperatures, the release rate and consumption of sulfur ions are so fast, leading to the formation of sulfur deficient copper sulfide $Cu_{1.65}S$.
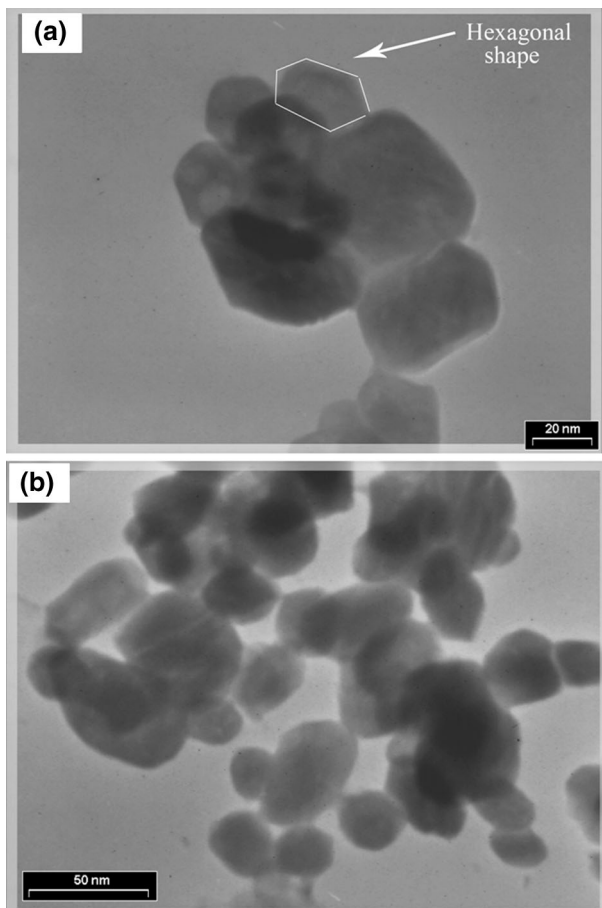
Fig. 2 TEM images of CuS nanoparticles synthesized with various Cu:S ratios: **a** 1:3 and **b** 1:5 at 105 °C for 60 min

Also, by increasing the reaction temperature to 200 °C, all reflections became sharper than the sample prepared at 105 °C. From Fig. 1c, the average crystallite size of ∼25 nm was obtained.

The ratios of the reagents, including the copper complex, surfactant, reaction temperature and reaction time, were effective parameters r controlling the size, shape and type of metal sulfide nanoparticles. The effect of copper:sulfur molar ratio on the particle size of the products is shown in Fig. 2. TEM images of copper sulfide nanoparticles synthesized at 105 °C with different copper:sulfur molar ratios of 1:3 and 1:5 have been shown in Fig. 2a, b. TEM images (see Fig. 2a, b) show that hexagonal nanoparticles were obtained in the case of copper:sulfur molar ratio of 1:3. By increasing copper:sulfur molar ratio from 1:3 to 1:5, the average particle size was increased from 20–45 to 25–50 nm (see Fig. 2b). With the comparison of the data shown in the SEM (Fig. 4a), TEM (Fig. 2a) images and XRD pattern (Fig. 1a), it was observed that h CuS *nanoparticles* were formed from relatively two or three *crystallites*. Furthermore, the shape of the product was changed from a hexagonal (Fig. 2a) morphology to a semi-spherical one (Fig. 2b).

Figure 3 shows the electron diffraction (ED) pattern of CuS nanoparticles synthesized at 105 °C with copper:sulfur molar ratios of 1:3. From inside to outside ring of the ED pattern, they were indexed to (100), (103), (006) and (105) of the hexagonal structure of polycrystalline CuS (Fig. 3a); this was consistent with the XRD data (Fig. 1).

To investigate the influence of the reaction time on the size of nanoparticles, it was varied from 60 min to 180 min (Fig. 4a–c) at 105 °C. As shown in Fig. 4a–c, upon increasing the reaction time from 60 min (the average size of 40–45 nm) to 180 min, agglomerated nanoparticles with the average size of 50–55 nm were yielded. It is well known that the synthesis of nanocrystals includes two steps:

Fig. 3 ED images of the as-synthesized copper sulfide synthesized with Cu:S ratio of 1:3 and at 105 °C for 60 min
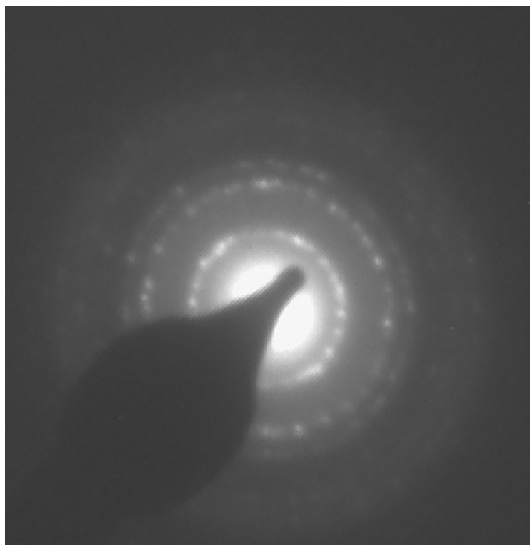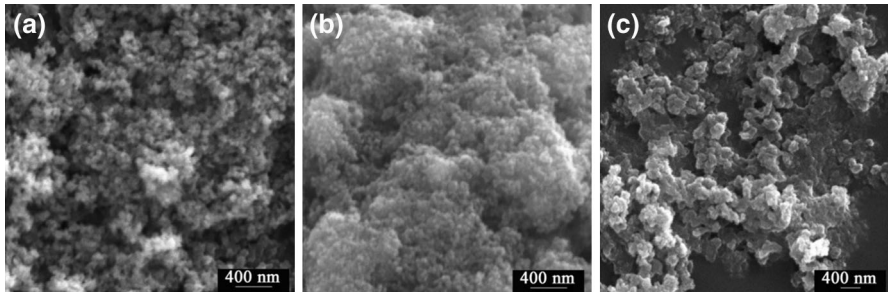
Fig. 4 SEM images of CuS nanoparticles formed with Cu:S ratio 1:3 for **a** 60 min, **b** 80 min and **c** 180 min

nucleation and growth. At the nucleating stage, the intrinsic crystal properties dominate the shape of the initial CuS seeds, that is, platelet hexagonal CuS seeds (Fig. 2). Subsequently, the precursors are absorbed to each plane, and the seeds grow. However, in this case, with increasing the reaction time, the rate of CuS seed growth was faster than nucleation step. Thus, CuS nanoparticles tended to grow in bigger sizes, as compared with lower reaction times (Fig. 4c).

To investigate whether the samples were capped with the organic surface, the Fourier transformed infrared (FT-IR) of the as-synthesized sample was performed. Figure 5 shows typical FT-IR spectra of CuS nanoparticles. The peaks at 2921 and 2857 cm^{-1} were due to the symmetric and asymmetric CH$_2$ stretching modes of oleylamine molecules. The peak at 3007 cm^{-1} was due to the n(C–H) mode of the C–H bond adjacent to the C=C bond and the small peak at 1624 cm^{-1} was due to the n(C=C) stretching mode of oleylamine molecules. The peak at 1591 cm^{-1} was
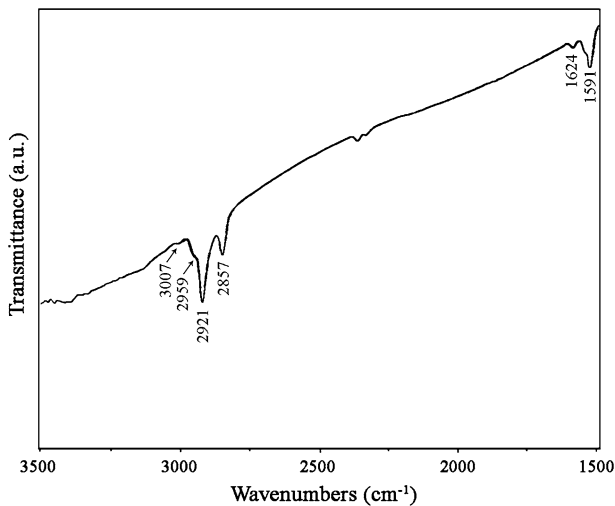
Fig. 5 Fourier transformed infrared (FT-IR) spectra of the as-synthesized CuS nanoparticles

UV-vis spectrum of the
as-synthesized copper sulfide
nanoparticles formed for 60 min
with Cu:S ratio *a* 1:3 and *b* 1:5
at 105 °C and *c* 1:3 at 200 °C
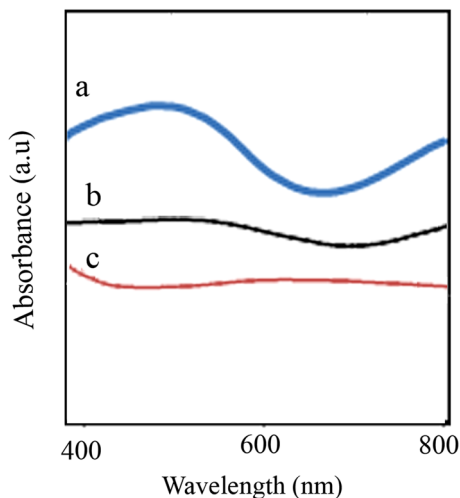
due to the $-NH_2$ scissoring mode. The results, therefore, clearly revealed that the
nanoparticles were coated with the oleylamine molecules [35].

The optical properties of copper sulfide nanoparticle were investigated at the
ambient temperature. The UV–Vis absorption spectra of copper sulfide nanopar-
ticles dispersed in ethanol have been in Fig. 6. According to the results obtained by
Dixit et al. [36, 37], the crystal phase of copper sulfide could be handily determined
from the absorption spectrum. Figure 6a shows a broad absorption band of sample
(a) formed with Cu:S ratio 1:3 at 105 °C for 60 min, at 500–650 nm. It can be
attributed to the d–d transition of Cu(II) state and is a general characteristic of
covellite phase [21, 33]. Compared with the absorption edge of the sample
(b) formed with the Cu:S ratio of 1:5 at 105 °C for 60 min, (Fig. 6b), there was a
blue shift in the sample (a). The result indicated that the CuS particles formed at
lower copper:sulfur molar ratio had a smaller size [17, 38, 39]. An obvious
absorption red-shift appeared in the sample (c) formed with the Cu:S ratio of 1:3 at
200 °C for 60 min, as shown in Fig. 6c, due to its larger particle size. Also, the
absorption of the sample prepared at 200 °C (Fig. 6c) showed a different absorption
profile. The band peak appeared around 400 nm with significantly reduced intensity
in near-IR region [40]. This confirmed the existence of sulfur deficient copper
sulfide, which was consistent with the XRD result (Fig. 1c). Research shows that at
temperatures below 180 °C, the CuS nanoparticle is covellite phase, while at
200 °C, it is digenite $Cu_{1.65}S$ phase [21, 33].

Conclusion

To summarize, hexagonal covellite (CuS) nanoparticles were successfully prepared
by tge thermal decomposition of a [Cu(sal)$_2$]- oleylamine complex in the presence
of elemental sulfur. By varying the key parameters, including the copper:sulfur

molar ratio, reaction temperature as well as the reaction time, we were able to prepare CuS nanoparticles with different average sizes and structures. Moreover, the imbalanced integration of copper ions and sulphur ions into a CuS cluster at high temperature could change the composition of the resulted nanoparticles. This occurred with increasing the reaction temperature from 105 to 200 °C. At this temperature, the phase of the samples was changed from covellite (hexagnal) to digenite (rhombohedral) structure. Moreover, upon increasing the reaction time from 60 min to 180 min, at 105 °C, the particle size of the CuS nanoparticle was increased from 40–45 to 50–55 nm due to the faster rate of CuS seed growth, as compared with nucleation.

References

1. J. Nezamifar, K. Ghani, and N. Kiomarsipour (2015). *J. Nanostruct.* **5**, 203–207.
2. Y. Wang, L. Zhang, H. Jiu, N. Li, and Y. Sun (2014). *Appl. Surf. Sci.* **303**, 54–60.
3. S. L. Prokopenko, G. M. Gunja, S. N. Makhno, and P. P. Gorbyk (2014). *J. Nanostruct. Chem.* **4**, 103–108.
4. S. Sagadevan, and K. Pandurangan (2015). *Int. J. Nano Dimens.* **6**, 433–438.
5. X. Wang, C. Xu, and Z. Zhang (2006). *Mater. Lett.* **60**, 345–348.
6. Y. Li, J. Scott, Y.-T. Chen, L. Guo, M. Zhao, X. Wang, and W. Lu (2015). *Mat. Chem. Phys* **162**, 671–676.
7. Y. Ni, F. Wang, J. Liu, Q. Miu, Z. Xu, and J. Hong (2003). *Chin. J. Inorg. Chem.* **19**, 1184–1197.
8. C. Nascu, I. Pop, V. Ionescu, E. Indrea, and I. Bratu (1997). *Mater. Lett.* **32**, 73–77.
9. M. Hossaini Sadr, and H. Nabipour (2013). *J. Nanostruct. Chem.* **3**, 26–31
10. F. Li, T. Kong, W. Bi, D. Li, Z. Li, and X. Huang (2009). *Appl. Surf. Sci.* **255**, 6285–6289.
11. V. Rajendran and J. Gajendiran (2015). *Mat. Sci. Sem. Proc.* **36**, 92–95.
12. Sh Sohrabnezhad, M. A. Zanjanchi, S. Hosseingholizadeh, and R. Rahnama (2014). *Spectrochim. Acta Part A* **123**, 142–150.
13. H. Zhu, X. Ji, D. Yang, Y. Ji, and H. Zhang (2005). *Microporous Mesoporous Mater.* **80**, 153–156.
14. A. Rahdar (2013). *J. Nanostruct. Chem.* **3**, 61–67.
15. A. K. Thottoli, and A. K. A. Unni (2013). *J. Nanostruct. Chem.* **3**, 56–62
16. D. Ghanbari, M. Salavati-Niasari, M. Esmaeili-Zare, P. Jamshidi, and F. Akhtarianfar (2014). *J. Ind. Eng. Chem.* **20**, 3709–3713.
17. J. Mohapatra (2013). *Int. Nano Lett.* **3**, 31–38.
18. T. H. Larsen, M. Sigman, A. Ghezeibash, R. C. Doty, and B. A. Korgel (2003). *J. Am. Chem. Soc.* **125**, 5638–5639.
19. S. Baskoutas, P. Giabouranis, S. N. Yannopoulos, V. Dracopoulos, L. Toth, A. Chrissanthopoulos, and N. Bouropoulos (2007). *Thin Solid Films* **515**, 8461–8464.
20. M. Salavati-Niasari, Z. Fereshteh, and F. Davar (2009). *J. Alloys Compd.* **476**, 797–801.
21. A. Ghezelbash and B. A. Korgel (2005). *Langmuir* **21**, 9451.
22. P. Zhang and L. Gao (2003). *J. Mater. Chem.* **13**, 2007.
23. H. Grijalra, M. Inoue, S. Boggavarapu, and P. Calvert (1996). *J. Mater. Chem.* **6**, 1157–1160.
24. P. P. Paul, T. B. Rauchfuss, and S. R. Wilson (1993). *J. Am. Chem. Soc.* **115**, 3316–3317.
25. J. Joo, H. B. Na, T. Yu, J. H. Yu, Y. W. Kim, F. Wu, J. Z. Zhang, and T. Hyeon (2003). *J. Am. Chem. Soc.* **125**, 11100–11105.
26. W. Lou, M. Chen, X. Wang, and W. Liu (2007). *J. Phys. Chem. C.* **111**, 9658–9660.
27. W. S. Seo, H. H. Jo, K. Lee, B. Kim, S. J. Oh, and J. T. Park (2004). *Angew. Chem. Int. Ed.* **43**, 1115–1117.
28. W. S. Seo, H. H. Jo, K. Lee, and J. T. Park (2003). *Adv. Mater.* **15**, 795–797.
29. W. P. Lim, C. T. Wong, S. L. Ang, H. Y. Low, and W. S. Chin (2006). *Chem. Mater.* **18**, 6170–6177.

30. H. T. Zhang, G. Wu, and X. H. Chen (2006). *Mater. Chem. Phys.* **98**, 298–303.
31. M. Salavati-Niasari and F. Davar (2009). *Mater. Lett.* **63**, 441–443.
32. H. Klug and L. Alexander *X-ray Diffraction Procedures* (Wiley, New York, 1962), p. 125.
33. Y. Liu, D. Qin, L. Wang, and Y. Cao (2007). *Mater. Chem. Phys.* **102**, 201–206.
34. S. K. Haram, A. R. Mahadeshwar, and S. G. Dixit (1996). *J. Phys. Chem.* **100**, 5868–5873.
35. B. Geng, X. Liu, J. Ma, and Q. Du (2007). *Mater. Sci. Eng. B* **145**, 17–22.
36. S. G. Dixit, A. R. Mahadeshwar, and S. K. Haram (1998). *Colloids Surf. A* **133**, 69–75.
37. L. Chu, B. Zhou, H. Mua, Y. Sun, and P. Xu (2008). *J. Cryst. Growth* **310**, 5437–5440.
38. M. Saranya, R. Ramachandran, E. J. J. Samuel, S. K. Jeong, and A. N. Grace (2015). *Powder Technol.* **279**, 209–220.
39. H. Qi, F. Huang, L.-Y. Cao, J.-P. Wu, and D.-Q. Wang (2012). *Ceram. Int.* **38**, 2195–2200.
40. Y. Cheng Chen, J. Bin Shi, C. Wu, C. Jung Chen, Y. Ting Lin, and P. Feng Wu (2008). *Mater. Lett.* **62**, 1421–1423.